Int. J. of GEOMATE, April, 2016, Vol. 10, No. 2 (Sl. No. 20), pp. 1770-1775
Geotech., Const. Mat. and Env., ISSN: 2186-2982(P), 2186-2990(O), Japan

SEISMIC EFFECTIVE STRESS ANALYSIS OF QUAY WALL IN LIQUEFIABLE SOIL: THE CASE HISTORY OF KOBE

Christos Souliotis[1] and Nikos Gerolymos[2]

[1,2]Faculty of Civil Engineering, National Technical University of Athens, Greece

ABSTRACT: During the previous decades, a significant number of failures of caisson quay walls have been observed. In particular, the majority of these failures are strongly connected to the deformational response of the surrounding (i.e. the backfill and the foundation) soil deposits subject to liquefaction. In this paper, the seismic effective stress analysis method is applied in order to investigate this complex phenomenon, through the use of the UBC3D-PLM constitutive model for stress-strain soil behaviour, which is available in the material library of the PLAXIS finite element code. An optimization procedure is presented for calibrating the parameters of the aforementioned constitutive model, which involves a two-step methodology based on matching: (a) the response of a single soil element under undrained monotonic direct simple shear loading reproduced by a recently developed more sophisticated model for sand, and (b) the cyclic resistance ratio curve in accordance with the NCEER/NSF procedure. The capability of the model in describing the response of a gravity-type quay wall undergoing lateral spreading due to soil liquefaction is then validated against a well-documented case history from the 1995 Kobe earthquake. The latter analysis is shown to reproduce satisfactory engineering accuracy in comparison to the observed response, shedding light to the validity of the proposed calibration methodology.

Keywords: Caisson Quay Walls, Finite Element Analysis, Liquefaction, Constitutive Model, Case History

1. INTRODUCTION

The dynamic response of gravity quay walls is strongly affected by non-linear soil behaviour. Development of excess pore pressures and accumulation of shear and volumetric strains, both at the retained and the foundation soil, produces shear strength degradation which may lead to liquefaction. The above phenomena are further complicated when accounting for soil-structure interaction. Evidently, the deformation modes that synthesize the response of the quay wall at large displacements and near failure conditions cannot be realistically assessed by conventional design procedures. The use of suitable constitutive soil models that balance simplicity and effectiveness in conjunction with powerful numerical techniques is a key-step for a successful prediction [1]–[3]. However, these more sophisticated procedures need to be verified before used in practice, and well-documented case histories can play a vital role on this.

In this paper, a methodology is developed for calibrating the model parameters of the UBC3D-PLM constitutive soil law [4], which is a 3D reformulation of that originally proposed by Puebla et al. [5] and Beaty and Byrne [6], designated as UBCSAND. The calibration procedure involves fitting the prediction of the model to: (i) undrained direct simple shear test results reproduced by a more sophisticated constitutive law by Tasiopoulou and Gerolymos [7], and (ii) the cyclic stress ratio (CRR) required to cause liquefaction (defined, either, from a threshold of excess pore water pressure ratio of $r_u = 0.98$, or, from a cyclic shear strain amplitude of $\gamma = 2.5\%$) in 15 uniform loading cycles [8], [9]. The case history of the caisson quay wall RC-5 in Rokko Island from the 1995 Kobe earthquake, whose large outward displacement and tilting have been documented and analysed by several researchers in a number of publications [2], [10], is then used as a benchmark for validating the capabilities of the calibrated constitutive soil model. The analysis, which is performed with the finite element code PLAXIS, is shown to reproduce satisfactory engineering accuracy in comparison to the observed response.

2. CONSTITUTIVE SOIL MODELLING

The UBC3-PLM model involves two yield surfaces (a primary and a secondary one) of the Mohr-Coulomb type. The primary surface evolves according to an isotropic hardening law, while a simplified kinematic hardening rule is used for the secondary yield surface. The elastic response is described by the elastic shear and bulk moduli given by:

$$G^e = K_G^e \cdot p_a \cdot (p/p_a)^{ne} \quad (1)$$

$$B^e = K_B^e \cdot p_a \cdot (p/p_a)^{me} \quad (2)$$

in which K_G^e and K_B^e are the elastic shear and bulk modulus numbers, p_a is the reference stress (usually the atmospheric pressure), p is the mean effective

stress and *ne*, *me* are exponents for stress dependency. The plastic shear modulus is given by:

$$G^p = G_i^p \cdot p_a \cdot \left(1 - \frac{n}{n_f} R_f\right)^2 \quad (3)$$

in which n is the current stress ratio, n_f is the stress ratio at failure, equal to $sin(\varphi_p)$, φ_p being the peak friction angle, and R_f is a failure ratio that truncates the hyperbolic curve. The plastic flow rule is non-associated and is based on the Drucker-Prager's law [11] and Rowe's stress dilatancy hypothesis [12]:

$$d\varepsilon_v^p = \left(sin(\phi_{cv}) - n\right) \cdot d\gamma^p \quad (4)$$

where $d\varepsilon_v^p$ and $d\gamma^p$ are the plastic volumetric and shear strain increments, respectively, φ_{cv} is the phase transformation friction angle, and G_i^p is a term that variates for primary, secondary and post-dilation loading and has the following form:

$$G_i^p = \frac{K_G^p}{p} \cdot \left(\frac{p}{p_a}\right)^{np} \cdot f\left(fac_{hard}, fac_{post}, n_{cyc}\right) \quad (5)$$

where K_G^p is the plastic shear modulus number, n_p is a constant exponent, and fac_{hard} is a parameter that controls the evolution (hardening) of the secondary yield surface to cyclic loading, as it affects the number of cycles (n_{cyc}) for liquefaction occurrence. The smaller the value of fac_{hard}, the greater the excess pore water pressure development and the lesser the liquefaction resistance is. On the other hand, fac_{post} governs the stiffness of soil after the onset of cyclic mobility, when the mobilized friction angle reaches the peak friction angle. The post-failure (at the onset of cyclic mobility) stiffness degradation increases with decreasing fac_{post}; the smaller the fac_{post}, the less stiff the post-failure response is.

3. CALIBRATION METHODOLOGY

The calibration methodology of the UBC3D-PLM constitutive model follows a two-step procedure. At first, the results from a series of single element undrained monotonic direct simple shear tests, predicted by the recently developed Tasiopoulou and Gerolymos model for sand [7], are matched with the help of a MATLAB optimization algorithm. The goal function is multi-objective, as the best fit to the τ-γ and τ-p' curves is concurrently attempted. In this step, all the parameters except from R_f, fac_{hard} and fac_{post} are optimized. The latter are then calibrated by fitting the cyclic resistance ratio curve corresponding to an earthquake magnitude of M = 7.5 (or 15 uniform loading cycles in terms of an element test), as proposed by Idriss and Boulanger [8], while keeping the rest of parameters constant, according to the formerly mentioned procedure.

The comparison of the predictions of the two aforementioned models, for relative density D_R = 25% and initial mean effective pressures p_0' = 100 kPa and p_0' = 500 kPa, is shown in Fig.1. The derived equations for the initially calibrated model parameters are summarized as follows:

$$K_G^e = 1592 \cdot D_R^{0.65} \quad (6)$$

based on the empirical formula derived by Seed and Idriss [13],

$$K_B^e = (2/3) \cdot K_G^e \quad (7)$$

$$ne = me = 0.5 \quad (8)$$

$$np = D_R \quad (9)$$

where, interestingly, the relative density D_R was found to be a very good estimator of the hardening exponent *np*, and

$$\phi_p - \phi_{cv} = 3.8 \cdot \left[D_R \cdot (9 - ln\, p_0') - 0.9\right] \geq 0 \quad (10)$$

It is observed that φ_{cv} is also a function of the initial mean effective stress, implying that layering during finite element modelling may not be avoided even for an initially uniform soil. However, it is pointed out that φ_{cv} in UBC3D-PLM plays the role of the phase transformation angle (φ_{pt}) rather than that of the critical state angle. Therefore, its pressure dependency for a given relative density is not surprising. Nevertheless, a constant value in the range of $32^o < \varphi_{cv} < 36.5^o$ could also be adopted for the sake of simplicity.

In addition, concerning the failure ratio parameter R_f, the initial generic calibrated expression of the UBCSAND model [14] is assumed, as in Eq. (11):

$$R_f = \frac{1}{(N_1)_{60}^{0.15}} \quad (11)$$

where $(N_1)_{60}$ is the corrected SPT blow-count, which is approximated as a function of the relative density D_R by using the empirical correlation of Idriss and Boulanger [8]:

$$(N_1)_{60} \approx 46 \cdot (D_R)^2 \quad (12)$$

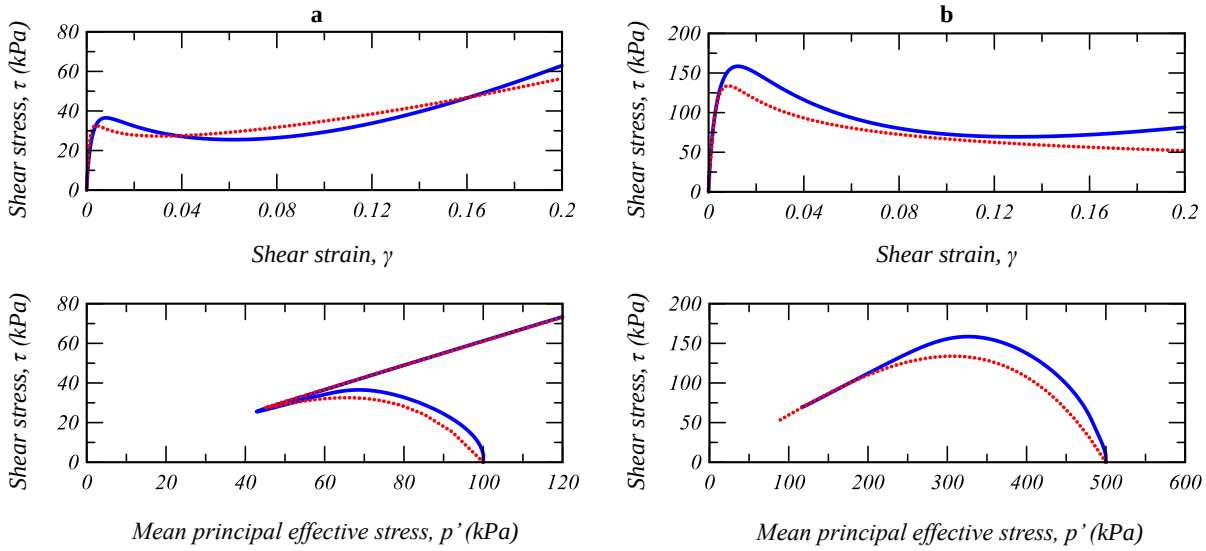

Fig.1 Comparison between the predictions of: (i) the Tasiopoulou and Gerolymos model for sand [7] (blue solid line) and (ii) the calibrated UBC3D-PLM constitutive model (red dotted line), for single element undrained monotonic direct simple shear tests of sand with D_R = 25%, and for initial mean effective pressures: (a) p_0' = 100 kPa and (b) p_0' = 500 kPa

The remaining parameters (i.e. K_G^p, fac_{hard} and fac_{post}) are derived based on the aforementioned two-step procedure, for a given relative density and an initial mean effective stress, after the initial estimation of those according to Eqs. (6) to (12).

The comparison between the cyclic resistance curve [8] and those predicted by the fully calibrated UBC3D-PLM model is shown in Fig.2.

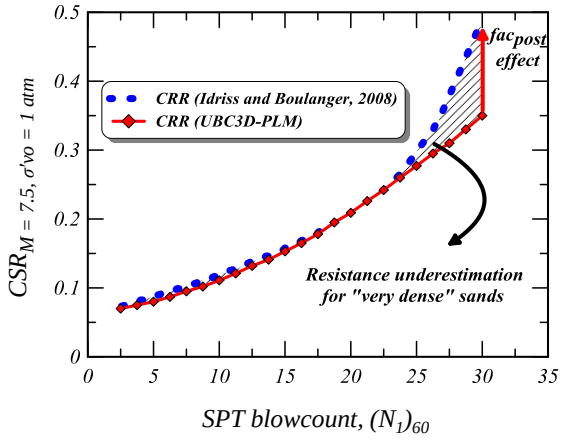

Fig.2 The CRR curve resulting from the calibration methodology. Resistance is underestimated for "very dense" sands, which can be counterbalanced by an increase in the fac_{post} parameter ("fac_{post} effect")

The corresponding values of fac_{hard} for different levels of the initial vertical effective stress as a function of $(N_1)_{60}$, as well as the predicted versus the empirically proposed K_σ effect [8] are provided in Fig.3. Finally, the prediction of the model in terms of cyclic undrained direct simple shear response is depicted in Fig.4, for two relative densities and for an initial vertical effective stress of 100 kPa. The results are presented in the form of excess pore water time history, stress-strain loop and effective stress path.

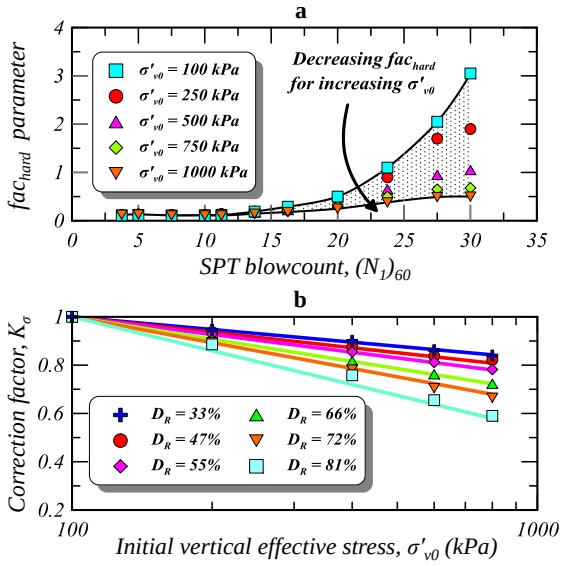

Fig.3 (a) The corresponding values of fac_{hard} for different levels of the initial vertical effective stress as a function of $(N_1)_{60}$, and (b) the predicted (discrete points) versus the empirically proposed (solid lines) K_σ effect [8]

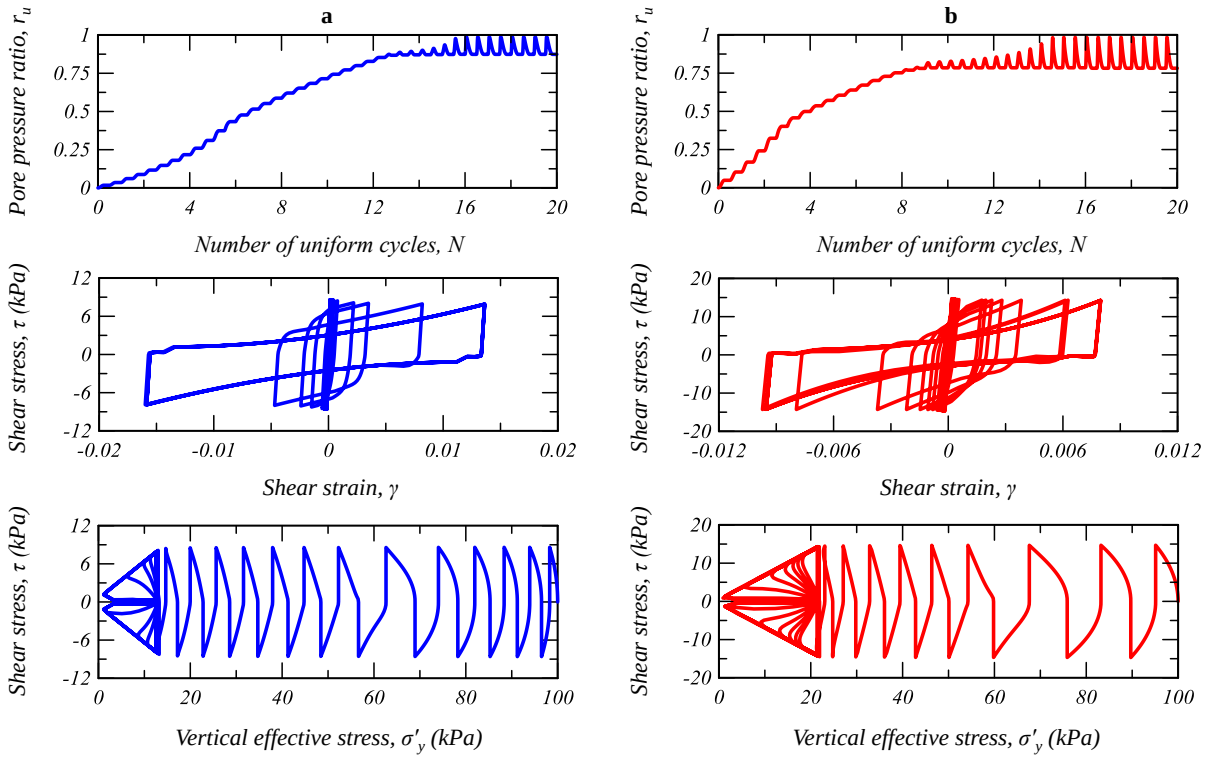

Fig.4 Prediction of the calibrated UBC3D-PLM model in terms of cyclic undrained direct simple shear response, for relative densities: (a) D_R = 33% and (b) D_R = 55%, and for an initial vertical effective stress of σ_{yo}' = 100 kPa

4. THE ROKKO ISLAND QUAY WALL

4.1 Field Observations

The case history corresponds to the typical quay wall section of Rokko Island, in which both the foundation and the backfill soil deposits are liquefiable. A cross-section of the quay wall with its deformation recorded after the earthquake is reproduced from Iai et al. [10] in Fig.5. During the earthquake the top of the wall moved about 4 m towards the sea (exceeding 5 m in a few locations) and experienced a settlement of approximately 1–2 m, tilting around 4° outwardly. Interestingly, there was no evidence of liquefaction occurrence either right behind the wall, at a distance of about 30 m, or near the toe of the wall in the sea [2]. Nevertheless, extensive liquefaction should have taken place farther away in the free field (see for examples [10], [15], [16]).

4.2 Numerical Model and Analysis

The seismic response of a typical section of the Rokko Island RC-5 quay wall is analysed with the use of the finite element code PLAXIS 2D AE. The finite element mesh and the material zones used in the analysis are shown in Fig.6, while the material properties are derived according to the previous calibration methodology (considering fac_{post} = 0.01 and φ_{cv} = 36°), for a given relative density D_R = 35% for the foundation and backfill soil deposits, and D_R = 40% for the rubbles. For simplicity (in order to avoid layering), the initial mean effective stresses are taken equal to p_0' = 100 kPa.

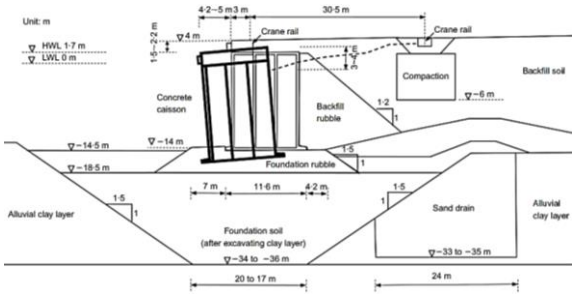

Fig.5 Cross-section of caisson quay wall RC-5 in Rokko Island and its residual deformation observed after Kobe 1995 earthquake [10]

Undrained effective stress analysis in the time domain is performed by taking into account for material (in the soil) and geometric (interface) nonlinearities. Both the quay wall and the soil are modelled with 15-node triangular plane strain elements, elastic for the former and nonlinear for the latter. The contact conditions between the quay wall and the adjacent soil are modelled with special inter-

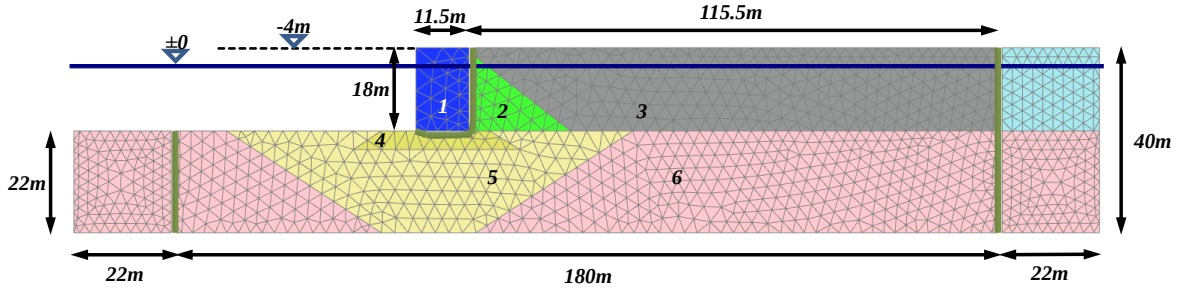

Fig.6 Finite element mesh with "free-field" elements at the sides [4]: (1) quay wall, (2) backfill rubble, (3) backfill soil, (4) foundation rubble, (5) foundation soil, and (6) alluvial clay

face elements, allowing for slippage and gapping via a Coulomb frictional law. The interface friction angles are assumed equal to 15° and 25° at the back and at the base of the wall, respectively. To avoid spurious oscillations at very small deformations and for high frequency components of motion, Rayleigh damping is also introduced into the model, accounting for equivalent hysteretic damping values between 1.5% and 3% in the range of 0.2-2 Hz. The initial horizontal effective stresses are set equal to 0.5 times the initial vertical effective stresses. The horizontal component (PGA = 0.54g) of the ground motion recorded in the nearby Port Island seismograph array (at the depth of 32 m) is used as the input motion at the base of the model [2]. Finally, "free-field" conditions are used for the outer boundaries in order to absorb wave reflections, as explained in depth in [4].

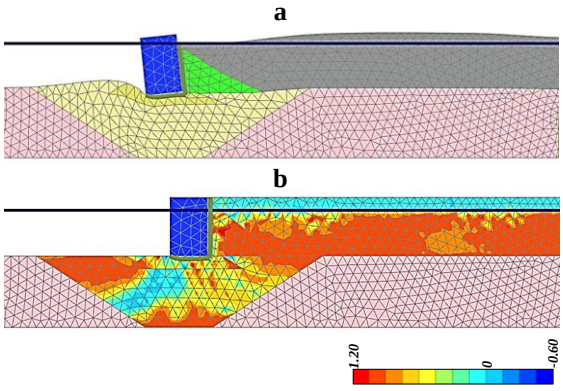

Fig.7 Snapshots of: (a) the deformed mesh and (b) the contours of the excess pore water pressure ratio, at the end of shaking

4.3 Results

The results of the effective stress analysis are presented in Figs.7 and 8 in the form of (i) snapshots of the deformed mesh and the contours of the excess pore water pressure ratio at the end of shaking, and (ii) time histories of the horizontal and vertical displacement and the tilt angle of the upper left corner of the wall.

Not only the observations regarding the residual displacements of the wall are satisfactorily reproduced, but the evidence regarding a zone of negative excess pore water pressure right behind the wall followed by extensive liquefaction at a farther distance, are also strongly supported. The above results lead to the conclusion that the proposed calibration methodology for the UBC3D-PLM constitutive soil model is satisfactory.

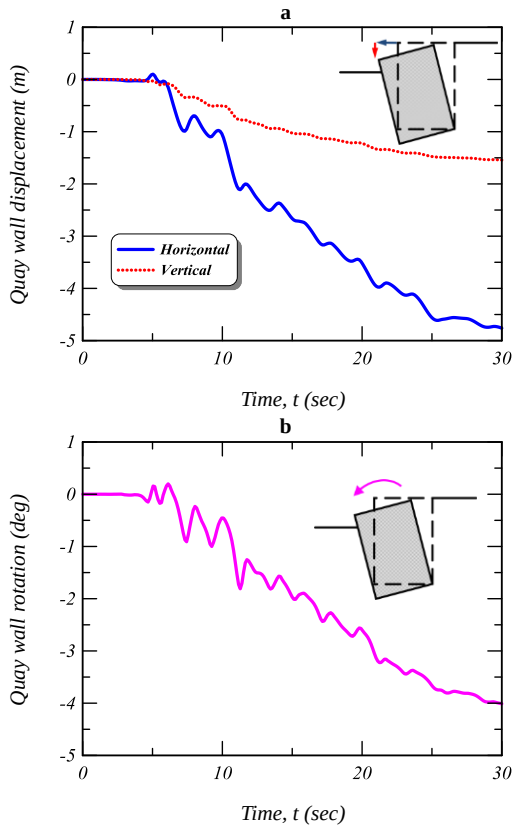

Fig.8 Computed time histories of: (a) the horizontal and vertical displacement and (b) the tilt angle, of the upper left corner of the wall (the negative sign denotes outward displacement and rotation)

5. CONCLUSION

This paper provides a detailed calibration methodology for the UBC3D-PLM constitutive soil model, which is available in the material library of the PLAXIS finite element code. The case history of the caisson quay wall RC-5 in Rokko Island from the 1995 Kobe earthquake, which suffered substantial outward displacement and rotation, has been utilized, by means of an undrained effective stress analysis in the time domain with the use of the aforementioned constitutive soil model, in order to evaluate the effect of the proposed calibration procedure. The predictions were shown to be in satisfactory agreement with the observed response, highlighting the validity of the present procedure for the initial estimation of the UBC3D-PLM model parameters.

6. ACKNOWLEDGEMENTS

This research has been financed by the Greek National State Scholarships Foundation (IKY) through the program "IKY Fellowships of Excellence for Postgraduate Studies in Greece – Siemens program".

7. REFERENCES

[1] Iai S, Matsunaga Y, Morita T, Miyata M, Sakurai H, Oishi H, Ogura H, Ando Y, Tanaka Y, Kato M, "Effects of remedial measures against liquefaction at 1993 Kushiro-Oki earthquake", in Proc. Fifth U.S.-Japan Workshop on Earthquake Resistant Design of Lifeline Facilities and Countermeasures against Soil Liquefaction, NCEER, 1994, pp. 135-152.

[2] Dakoulas P, Gazetas G, "Insight into seismic earth and water pressures against caisson quay walls", Géotechnique Vol. 58, No. 2, 2008, pp. 95–111.

[3] Byrne P, Park SS, Beaty M, Sharp M, Gonzalez L, Abdoun T, "Numerical modeling of liquefaction and comparison with centrifuge tests", Canadian Geotechnical J. Vol. 41, 2004, pp. 193-211.

[4] Galavi V, Petalas A, Brinkgreve RBJ, "Finite element modeling of seismic liquefaction in soils", Geotechnical Engineering Journal of the SEAGS & AGSSEA, Vol. 44, No. 3, 2013, pp. 55-64.

[5] Puebla H, Byrne PM, Phillips R, "Analysis of CANLEX Liquefaction Embankments: Prototype and Centrifuge Models", Canadian Geotechnical J., Vol. 34(5), 1997, pp. 641-657.

[6] Beaty M, Byrne P, "An effective stress model for predicting liquefaction behaviour of sand", Geotechnical Earthquake Engineering and Soil Dynamics III, ASCE Geotechnical Special Publication, No. 75, 1998, pp. 766-777.

[7] Tasiopoulou P, Gerolymos N, "Constitutive modeling for sand with emphasis on the evolution of bounding and phase transformation lines", in Proc. of the 8th European Conference on Numerical Methods in Geotechnical Engineering, Delft, the Netherlands, 18-20 June 2014, pp. 109-114.

[8] Idriss IM, Boulanger RW, "Soil liquefaction during earthquakes", Monograph MNO-12, Earthquake Engineering Research Institute, Oakland, CA, 2008, pp. 261.

[9] Youd TL, Idriss IM, "Liquefaction resistance of soils: summary report from the 1996 NCEER and 1998 NCEER/NSF workshops on evaluation of liquefaction resistance of soils", Journal of Geotechnical and Geoenvironmental Engineering, Vol. 127, No. 4, April. 2001, pp. 297-313.

[10] Iai S, Ichii K, Liu H, Morita T, "Effective stress analysis of port structures", Soils Found. (Special issue on geotechnical aspects of the January 17, 1995 Hyogoken-Nambu earthquake), Vol. 2, 1998, pp. 97-114.

[11] Drucker DC, Prager W, "Soil mechanics and plastic analysis for limit design", Quart. Appl. Math., Vol. 9, 1952, pp. 381-389.

[12] Rowe PW, "The stress-dilatancy relation for static equilibrium of an assembly of particles in contact", in Proc. of the Royal Society of London, Mathematical and Physical Sciences, Series A, Vol. 269, 1962, pp. 500-557.

[13] Seed HB, Idriss IM, "Soil moduli and damping factors for dynamic response analyses", Report EERC No 70-100, Earthquake Engineering Research Center, University of California, Berkeley, 1970.

[14] Beaty M, Byrne P, "UBCSAND constitutive model, Version 904aR", Documentation Report: UBCSAND constitutive model on Itasca UDM Web Site, 2011, pp. 69.

[15] Towhata I, Ghalandarzadeh A, Sundarraj K, Vargas-Monge W, "Dynamic failures of subsoils observed in waterfront areas", Soils Found. (Special issue on geotechnical aspects of the January 17, 1995 Hyogoken-Nambu earthquake), Vol. 1, 1996, pp. 149-160.

[16] Inagaki H, Iai S, Sugano T, Yamazaki H, Inatomi T, "Performance of caisson type quay walls at Kobe port", Soils Found. (Special issue on geotechnical aspects of the January 17, 1995 Hyogoken-Nambu earthquake), Vol. 1, 1996, pp. 119-136.

Int. J. of GEOMATE, April, 2016, Vol. 10, No. 2 (Sl. No. 20), pp. 1770-1775.

MS No. 41901 received on Oct. 16, 2015 and reviewed under GEOMATE publication policies.

Corresponding Author: Christos Souliotis